



Publication Year	2022
Acceptance in OA	2025-03-24T15:40:29Z
Title	The small-sized telescope of CTAO
Authors	TAGLIAFERRI, Gianpiero, Antonelli, A., Arnesen, T., Aschersleben, J., ATTINA', Primo, Balbo, M., Bang, S., Barcelo, M., Baryshev, A., BELLASSAI, Giancarlo, Berge, D., Bicknell, C., BIGONGIARI, Ciro, BONNOLI, Giacomo, Bouley, F., Brown, A., BULGARELLI, ANDREA, CAPPI, MASSIMO, CARAVEO, Patrizia, CASCHERA, Salvatore, Chadwick, P., Conte, F., Cotter, G., Cristofari, P., De Frondat, F., De Gouveia Dal Pino, E., De Simone, N., Depaoli, D., Dournaux, J. -L., Duffy, C., Einecke, S., Fermino, C., Funk, S., GARGANO, Carmelo, Giavitto, G., GIULIANI, Andrea, Greenshaw, T., Hinton, J., Huet, J. -M., Iovenitti, S., LA PALOMBARA, NICOLA, Lapington, J., Laporte, P., Leach, S., LESSIO, Luigi, LETO, Giuseppe, Lloyd, S., LUCARELLI, Fabrizio, LOMBARDI, Saverio, Macchi, A., MARTINETTI, Eugenio, MICCICHE', Antonio, MILLUL, Rachele, MINEO, TERESA, Mitsunari, T., Nayak, A., NICOTRA, Gaetano, Okumura, A., PARESCI, Giovanni, Penno, M., Prokoph, H., Rebert, E., RIGHI, Chiara, Rulten, C., RUSSO, Federico, Sanchez, R. Zanmar, SATURNI, Francesco Gabriele, Schaefer, J., Schwab, B., SCUDERI, Salvatore, SIRONI, Giorgia, Sliusar, V., Sol, H., Spencer, S., STAMERRA, Antonio, Tajima, H., TAVECCHIO, Fabrizio, Tosti, G., TROIS, Alessio, Vecchi, M., VERCELLONE, Stefano, Vink, J., Walter, R., Watson, J., White, R., Zanin, R., ZAMPIERI, Luca, Zech, A., Zink, A.
Publisher's version (DOI)	10.1117/12.2627956
Handle	http://hdl.handle.net/20.500.12386/36937
Serie	PROCEEDINGS OF SPIE
Volume	12182

The Small-Sized Telescope of CTAO

G. Tagliaferri^{1a}, A. Antonelli^b, T. Arnesen^c, J. Aschersleben^c, P. Attinà^a, M. Balbo^d, S. Bang^e, M. Barcelo^f, A. Baryshev^c, G. Bellassai^g, D. Berge^h, C. Bicknell^s, C. Bigongiari^b, G. Bonnoli^a, F. Bouleyⁱ, A.M. Brown^j, A. Bulgarelli^k, M. Cappi^k, P. Caraveo^l, S. Caschera^m, P. Chadwick^j, F. Conte^f, G. Cotterⁿ, P. Cristofariⁱ, F. De Frondatiⁱ, E. De Gouveia Dal Pino^o, N. De Simone^h, D. Depaoli^f, J.-L. Dournauxⁱ, C. Duffyⁿ, S. Einecke^p, C. Fermino^o, S. Funk^q, C. Gargano^r, G. Giavitto^h, A. Giuliani^l, T. Greenshaw^r, J. Hinton^f, J.-M. Huetⁱ, S. Iovenitti^a, N. La Palombara^l, J. Lapington^t, P. Laporteⁱ, S. Leach^t, L. Lessio^u, G. Leto^g, S. Lloyd^d, F. Lucarelli^b, S. Lombardi^b, A. Macchi^a, E. Martinetti^g, A. Miccichè^a, R. Millul^a, T. Mineo^r, T. Mitsunari^e, A. Nayak^j, G. Nicotra^g, A. Okumura^e, G. Pareschi^a, M. Penno^h, H. Prokoph^h, E. Rebertⁱ, C. Righi^a, C. Rulten^j, F. Russo^k, R. Zanmar Sanchez^g, F.G. Saturni^b, J. Schaefer^q, B. Schwab^q, S. Scuderi^l, G. Sironi^a, V. Sliusar^d, H. Soliⁱ, S. Spencer^q, A. Stamerra^b, H. Tajima^e, F. Tavecchio^a, G Tosti^{a,x}, A. Trois^m, M. Vecchi^c, S. Vercellone^a, J. Vink^v, R. Walter^d, J. Watson^h, R. White^f, R. Zanin^w, L. Zampieri^u, A. Zechⁱ, A. Zink^q

^aINAF-Osservatorio Astronomico di Brera, Merate, Italy; ^bINAF-Osservatorio Astronomico di Roma, Monteporzio, Italy; ^cKapteyn Astronomical Institute, University of Groningen, Groningen, The Netherlands; ^dUniversity of Geneva, Geneva, Switzerland; ^eNagoya University, Nagoya, Japan; ^fMax Planck Institute for Nuclear Physics, Heidelberg, Germany; ^gINAF-Osservatorio Astrofisico di Catania, Catania, Italy; ^hDeutsches Elektronen-Synchrotron, Zeuthen, Germany; ⁱObservatoire de Paris-PSL, CNRS, Meudon, France; ^jDurham University, Durham, UK; ^kINAF-Osservatorio Astrofisica e Scienza dello Spazio, Bologna, Italy; ^lINAF-Istituto di Astrofisica Spaziale, Milano, Italy; ^mINAF-Osservatorio Astronomico di Cagliari, Selargius, Italy; ⁿUniversity of Oxford, Oxford, UK; ^oIAG-University of Sao Paulo, Sao Paulo, Brazil; ^pThe University of Adelaide, Adelaide, Australia; ^qECAP Friedrich-Alexander-Universität Erlangen-Nürnberg, Erlangen, Germany; ^rINAF-Istituto di Astrofisica Spaziale, Palermo, Italy; ^sThe University of Liverpool, Liverpool, UK; ^tThe University of Leicester, Leicester, UK; ^uINAF-Osservatorio Astronomico di Padova, Padova, Italy; ^vUniversity of Amsterdam, Amsterdam, The Netherlands; ^wCherenkov Telescope Array Observatory, Bologna, Italy; ^xUniversità degli Studi di Perugia, Perugia, Italy.

ABSTRACT

The Cherenkov Telescope Array Observatory (CTAO) consists of three types of telescopes: large-sized (LST), medium-sized (MST), and small-sized (SST), distributed in two observing sites (North and South). For the CTA South “Alpha Configuration” the construction and installation of 37 (+5) SST telescopes (a number that could increase up to 70 in future upgrades) are planned. The SSTs are developed by an international consortium of institutes that will provide them as an in-kind contribution to CTAO. The SSTs rely on a Schwarzschild-Couder-like dual-mirror polynomial optical design, with a primary mirror of 4 m diameter, and are equipped with a focal plane camera based on SiPM detectors covering a field of view of $\sim 9^\circ$. The current SST concept was validated by developing the prototype dual-mirror ASTRI-Horn Cherenkov telescope and the CHEC-S SiPM focal plane camera. In this contribution, we will present an overview of the SST key technologies, the current status of the SST project, and the planned schedule.

Keywords: gamma-ray astronomy, CTA project, Cherenkov Telescope, dual-mirror Schwarzschild-Couder design, SiPM detector

¹ corresponding author: gianpiero.tagliaferri@inaf.it; phone +39-02-72320-433; www.brera.inaf.it

1. INTRODUCTION

To provide a high imaging sensitivity over an extensive energy range, from a few tens of GeV up to a few hundreds of TeV, the Cherenkov Telescope Array Observatory (CTAO, see web page link at <https://www.cta-observatory.org> and reference [2]) will be made of sub-arrays with three different types of telescopes: large-sized (LST, 23 m diameter [1]), medium-sized (MST, 12 m diameter [3]) and small-sized (SST, 4 m diameter) telescopes. They are distributed in two observing sites, the Northern one in La Palma, the Canary Islands, and the Southern one in the Chilean Andes in the Paranal area. The CTA South “Alpha Configuration” would include both MSTs and SSTs, with the possibility of including also LSTs in a second moment. In particular, it envisages the construction and installation of 37 SSTs (a number that could increase up to 70 in future upgrades). A proposal submitted to the Italian national recovery plan program in February 2022 has just been approved (at the time of the writing of this paper). It foresees the construction of two LSTs and 5 more SSTs, to be installed at the Southern site.

The SST is an imaging atmospheric Cherenkov telescope (IACT). Cherenkov telescopes use the Earth’s atmosphere as a detection medium and provide a collecting area large enough to detect, indirectly, the very-high-energy (VHE) gamma rays in the GeV-TeV energy band. In particular, the SSTs are sensitive in the band from ~ 0.5 TeV up to ~ 300 TeV, providing the system sensitivity to the highest energies. When a VHE gamma-ray interacts with the atoms and ions in the upper levels of the atmosphere, it induces a cascade of secondary particles which propagate over many kilometres at nearly the speed of light through the atmosphere. These particles emit Cherenkov light, forward-beamed with an opening angle of about one degree. When a cascade originates at an altitude of 10 km from the telescopes it illuminates a light pool on the ground of about 120 m radius. IACT telescopes collect Cherenkov light produced by secondary charged particles and obtain an image of the particle cascade employing an imaging camera designed specifically to detect such Cherenkov light. A Cherenkov shower event consists of a time-correlated multi-photon image with a typical timescale of ~ 10 ns.

The SSTs are developed by an international consortium of institutes that will provide them as an in-kind contribution to CTAO. The SST program for the provision of the 37 (+5) SSTs is organised around two main projects: the SST-STR (mechanical structure mated with the optics) and the SST-CAM (the camera to be mounted at the focal plane of the optical system). The SST-STR relies on a modified Schwarzschild-Couder dual-mirror optical design, where the mirror profiles have been optimised adopting a polynomial solution, to provide a good spatial resolution over a large field of view [14]. The SST has a primary mirror of ~ 4 m diameter, made of 18 hexagonal segments with a total aperture of 4.3 m. The SST telescope is made by equipping the SST-STR with the SST-CAM: a focal plane camera based on an array of SiPM detectors covering a field of view of $\sim 9^\circ$. In the following sections, we will present an overview of the SST key technologies, the ongoing activities for the final consolidation of the SST design, and the planned time schedule for the implementation of the array.

2. DESCRIPTION OF THE SST PROJECT

2.1 The current status of the project

The current SST configuration was finally selected in summer 2020 by CTAO as the baseline configuration, following the successful development of both a prototype Schwarzschild-Couder-like Cherenkov telescope with polynomial optical design (named ASTRI-Horn [4]) and a SiPM focal plane camera (CHEC-S [5]).

The telescope validation was achieved making a characterisation of the aplanatic behaviour of the ASTRI-Horn optical system across the entire field of view by using an optical camera [6], followed by the detection of the emission from the Crab nebula using a camera developed by the ASTRI consortium [7]. This test represents the first astronomical observation of gamma-rays using an IACT dual mirror system. In parallel, the CHEC-S camera prototype was developed and subjected to functional tests. Finally, the CHEC-S camera was integrated on ASTRI-Horn, and Cherenkov signals were detected as expected [8].

The overall telescope properties are summarised in Table 1.

Table 1. overall main properties of the Small-Sized telescope (SST)

Small-Sized Telescope (SST)	
Optical Design	modified Schwarzschild-Couder
Primary reflector diameter	4.3 m
Secondary reflector diameter	1.8 m
Effective mirror area (including shadowing)	>5 m ²
Focal length	2.15 m
Total weight	17.5 t
Field of view	8.8 deg
Number of pixels in SST-CAM	2048
Pixel size (imaging)	0.16 deg
Photodetector type	SiPM
Telescope data rates (before array trigger)	>600 Hz
Telescope data rates (readout of all pixels; before array trigger)	2.6 Gb/s
Positioning time to any point in the sky (>30° elevation)	90 s
Pointing Precision	< 7 arcsecs

While waiting for the final formalisation of the CTAO ERIC (European Research Infrastructure Consortium, expected to occur by the end of 2022 and that will be the governing legal entity of CTAO), we are now in a “Bridging Phase” that started in July 2021 and will be completed by the end of December 2022. These activities have been programmed following the Design and Value Engineering Review (DVER) carried out in summer 2020. The implementation of the recommendations after this review represents the final step of the SST harmonisation process that led to its final configuration after the development of some prototypes.

Following the outcome of the DVER process, an SST international consortium has been created to deliver the SST array as an in-kind contribution to CTAO. This consortium currently includes 15 Institutes from Italy, France, Germany, UK, Switzerland, Netherlands, Japan, Australia, and Brazil, and it is open to the inclusion, where possible, of more participants from the wider CTA community. The INAF institute from Italy is coordinating the Consortium's activities and chairing the SST Executive Steering Committee in charge of the overall supervision of the program. INAF also provide the Project Manager for the comprehensive SST program.

During the current phase, we are addressing the critical points and defining the activities to be pursued before the production and implementation phase. The latter will take place after the ERIC has formally started. The outcome will be the final design of the SST and the final set of documents that will be the input for the implementation phase of the SST array (37+5 telescopes).

In summary, the overall project timeline is divided in four main phases:

- Bridging
- Design Consolidation
- Production
- AIV (Assembly, Integration and Verification)

Bridging Phase. This is the ongoing phase in which the design of the SST structure (SST-STR, based on the ASTRI structure), the SST Camera (SST-CAM, based on the CHEC-S camera), and SST Optics will be iterated to define the final SST Telescope design. The Bridging Phase closing is foreseen by the end of 2022.

Design Consolidation Phase. During this phase, there will be the final release of Level B requirements by CTAO and the assessment of lower-level Requirements from the SST Consortium. The outcoming of this phase is the final SST design, optimised for simplicity, reliability, maintainability, and cost. This phase also sees the production of plans and documentation for the Production and AIV Phase. The Design Consolidation Phase is expected to take 1.5-2 years.

Production Phase. In this phase, the SST Partners will produce the elements of the SSTs (Structures, Cameras, and Optics), to be delivered to the CTAO Southern site over approximately 2.5 years. The Production Phase ends with the delivery of the last set of elements to the Southern site.

AIV Phase. It will start when the first telescope is available on site. The delivered products will be installed and integrated on the foundation prepared by CTAO. Each telescope will be commissioned and handed over to CTAO. Due to the large number of telescope units, Telescope Production and AIV phases will be run in parallel. The AIV phase will end with the acceptance of the final set of SSTs by CTAO (~3.5 years from phase start).

We will now describe the three main hardware components of the telescope: the Structure, the Camera and the Optics.

2.2 The mechanical structure

The current structure baseline selected for the SST (SST-STR) is the outcome of a project initiated in 2011 as a “flagship project” funded by the Italian Ministry of University and Scientific Research (MUR). This project is named ASTRI and was led by INAF. It started with developing a prototype Cherenkov telescope of the 4-m class, relying on an innovative dual-mirror optical configuration based on a polynomial-modified Schwarzschild - Couder design previously proposed by Vassiliev et al., [9], for IACT telescopes. The Italian ASTRI team developed this telescope as a technological demonstrator in the context of the development of the SST project for CTAO in its early phase. In 2014 it was installed on the Mount Etna volcano, at the M.G. Fracastoro astronomical station operated by INAF–Osservatorio Astrofisico di Catania (see Figure 1, and [10]). This prototype has been named ASTRI-Horn after Guido Horn D’Arturo, the astronomer who pioneered the segmented mirrors approach for the realisation of primary mirrors of large diameter telescopes. The ASTRI-Horn is now available as a test bench for implementing hardware and software developed by the SST team.

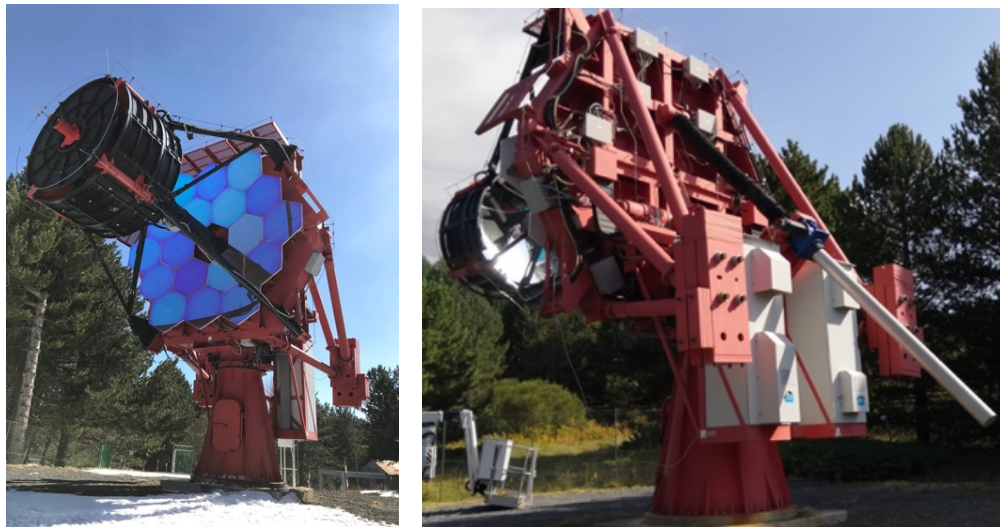


Figure 1. The ASTRI-Horn telescope prototype on the Mount Etna station of the INAF-Osservatorio Astrofisico di Catania

Following the successful realisation of the ASTRI-Horn prototype, the ASTRI team moved toward implementing 9 other telescopes, named the ASTRI Mini-Array [11]. This mini-array was supposed to be a pathfinder for the Southern site of CTAO, also representing the first seed around which the SST array would have been developed. However, the ASTRI timeline, dictated by the funds' availability and time-frame in which they had to be spent, was ahead of the CTAO site-building timeline. Therefore, in 2019 INAF and the Instituto de Astrofisica de Canarias (IAC) agreed to install the ASTRI Mini-Array at the Teide Astronomical Observatory in the Canary Islands of Tenerife.



Figure 2 left: a 3-D model of the SST telescope structure; right: the first ASTRI Mini-r-ray telescope fully assembled in a warehouse in Italy before being shipped to the Tenerife Canary Island. This is also the baseline of the SST telescopes, currently under study for further possible improvements.

Taking advantage of the lessons learned during the development and operations of the ASTRI-Horn prototype, the design of the ASTRI Mini-Array electro-mechanical structure has been further optimised (see Figure 2 left panel), and in Autumn 2020, CTAO defined this to be the SST structure baseline configuration. In this optimization, the mass has been reduced by ~5 tons (from 22 to 17 tons) while the stiffness has either been maintained or improved for some aspects. The structure supporting the segments of the primary mirror (M1 dish) and the system supporting the secondary mirror (M2) were deeply revisited, improving their functionality, reliability, and maintainability, besides making them lighter. For a detailed description of these improvements, see [11][12]. The electromechanical structure of the first ASTRI Mini-Array telescope has now been constructed and fully integrated at the EIE GROUP srl company warehouse in Mira, near Venice (Italy, see Figure 2, right panel). Then it has been dismantled, and shipped to Tenerife (Canary Islands) and has been integrated at the Teide Astronomical Observatory (see Lombardi et al. this conference).

Given the strong commonality that there is between the ASTRI Mini-Array and the SST Array and that the ASTRI team is largely present also in the SST team, we are directly experimenting all procedures necessary for the fabrication, integration, verification, shipment of the telescope from Europe to the remote observing site, on-site integration and related AIV/AIT (Assembly, Integration, Verification and Testing) activities. That is, we are directly proving all the steps necessary to go from a telescope design to a fully mounted and working telescope at the observing site. This allows us to put the construction of the SST array on a very solid basis.

As said, the original ASTRI-Horn M1 dish has been significantly modified. Now for the ASTRI Mini-Array it is made in two parts, simplifying its transportation to the Observatory site and its onsite integration. Given that this has to be done for more than 40 telescopes, it has an important impact on the onsite AIV/AIT activities. Also, the way to support the M1 segments has significantly changed. The current layout provides complete modularity of the segment supports, which are reduced to only 3 types, compared to the 18 types before. This has been obtained by using a cylindrical symmetry, while before the position was based on Cartesian coordinates. With this configuration, the M1 segment integration and alignment is achieved in less than one day. Still, during the current Bridging Phase, we are looking into the M1 dish to see if it is possible to improve its design even further, see next section.

M1 dish optimisation

Although the baseline M1 dish already satisfy the requirement given for the SST, we are in any case looking for further possible improvements of this sub-component. A team from the Observatoire de Paris-Meudon/CNRS leads these studies for a possible optimization of the M1 dish design, assuming that interfaces and global philosophy must stay the same. For this purpose, an optimised design process, based on structural optimization tools, is used. This process allows us to reduce required iterations between the computer aided design (CAD) and the finite element analysis (FEA). This work is based on previous experiences of the French team in this field, namely for mechanical studies for CTAO SST before the selection of the ASTRI design after the DVER. This optimization focuses on the redefinition of the beam layout of the M1 dish. The mechanical interfaces with the elevation fork, the M1 segments, the counterweights of the optical support structure, the AIT and shipping philosophies are kept. The SOL 200 of the Nastran FEA code has been used to carry out the optimization study. The details on the performed process and achieved results are detailed in another conference paper [13].

The combined use of topology and topography optimization, a kind of shape optimization, and post-processing of these results allowed us to obtain a different beam layout, as shown in Figure 3.

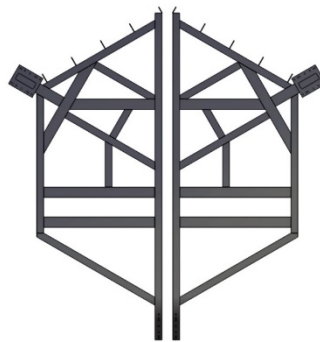


Figure 3. Main beam layout of the alternative design.

A second step of the work consisted in defining the geometry of the sections of these beams. The choice was to adopt standard U and I profiles for the beams, in order to make easier the fabrication process. The resulting 3D design is shown in Figure 4.

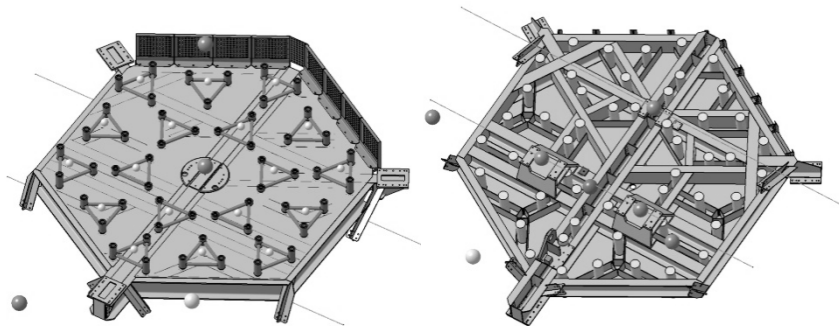


Figure 4. Alternative conceptual design of the M1 Dish.

The performances of this design are compared to the performances of the baseline first in terms of mass and mechanical behaviour (stress and displacement linear static analyses and normal modes). The mechanical performance has been preliminary evaluated by finite-element analyses by using the SOL 101 and SOL 103 packages of Nastran. As a result, this design is slightly lighter than the ASTRI dish baseline and allows a significant increase in the first eigenfrequency, that imply an increase of the robustness to the earthquake accelerations, with also an important decrease of the Von Mises stress, that allows a higher safety factor to yield stress of the materials. The alternative design seems to have also a low impact on the displacements of the M1 segments, that is directly correlated to the optical quality of the image. Table 2 and Table 3 summarise the achieved results.

Table 2. Comparison of the two designs.

	Baseline	Alternative
Mass (kg)	3 004	2 859
1 st eigenfrequency (Hz)	57,4	93,4
Max Von Mises stress @0° (MPa)	11,9	2,8

Table 3. Average displacements and rotations of M1 panels Centre of Gravity for the two designs (elevation angle).

	Decentre (µm)	Defocus (µm)	Tilt x (µrad)	Tilt y (µrad)
0 degree				
Baseline	4,5	0,3	3,1	-0,1
Alternative	5,4	1,1	2,8	0,2
90 degrees				
Baseline	1,7	12,6	-7,0	0,1
Alternative	1,5	7,7	-0,7	0,2

Performances are the same for both designs in static analysis but there is a clear improvement for the dynamic analysis. On the other hand, this alternative solution has to show a proper performance to sustain the demanding seismic load that is required to the SSTs in Chile. For this reason, the alternative proposed design is currently being injected in the global design for the seismic analysis to have the complete FEA comparison between both solutions. Based on the outcome of this analysis, a trade-off comparison will be made between the baseline and this alternative solution in order to make the final selection for the M1 dish configuration, evaluating also the different implementation costs that the two solutions (baseline and alternative design) may have. This is expected to occur within the next 1-2 months.

2.3 The optics system

The SST optical design is based on compact classical altitude-azimuth configuration, adopting a slightly modified dual-mirror Schwarzschild-Couder configuration (see Figure 5). Unlike the Dennis-Cotton configuration that has a spherical mirror profile, as in the case of the MST and LST telescopes, the SST mirror profile is aplanatic and it is described by an aspherical polynomial function (see [14]) that allows us to derive a good imaging capability over a larger field of view (while it introduces a small on-axis degradation with respect to the classical Schwarzschild-Couder design). Such a configuration can be obtained even for small focal ratios, facilitating the construction of compact telescopes and overall camera size. In the case of SST, the focal ratio is $F=0.5$ with a plate scale of $37.5 \text{ mm}/^\circ$. Given that the Cherenkov pixel is approximately 0.16° , with an equivalent focal length of 2155 mm the SST optical design provides a usable field of view of $\sim 9.5^\circ$ in diameter and an effective area of $\sim 5 \text{ m}^2$.

The 4.3 m diameter primary mirror is segmented following the scheme reported in Figure 5. The full reflector comprises 18 segments (the central one is not used). The segmentation requires three segments with different surface profiles identified with different colours in the figure. The segments have a hexagonal shape with a face-to-face size of 85 cm. A 9 mm gap separates each segment from the next one to facilitate the mounting and alignment operations.

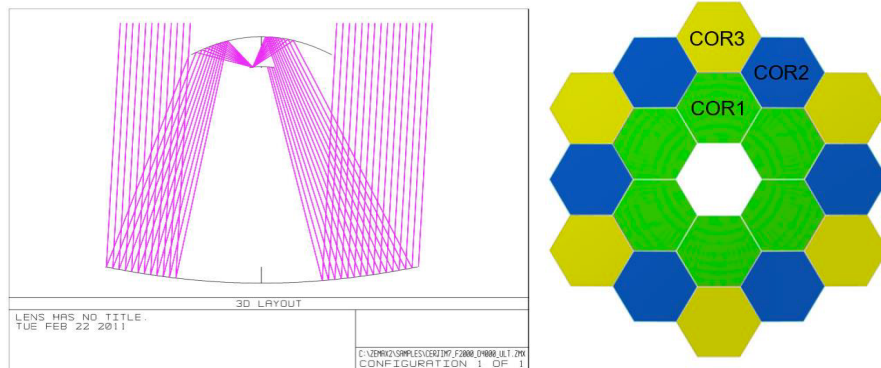


Figure 5 left: the SST optical system; right: tessellation of the primary mirror M1; the 18 segments are divided into three groups, identified by the colours, with a different shape.

Each segment is equipped with three actuators, to correct for the tip/tilt and piston misplacements of each element. An active alignment system (actuators, controls, etc) will be installed only during the integration; after the mirrors have been aligned, the dynamic system is removed, and only a passive fixed system will be in place. The active system can be used again every time the mirror system will need to be aligned, but this is estimated to be necessary very rarely. The segments of the primary mirror are realised using a glass cold-slumping technology, the proper mirror shape is obtained by bending a thin glass foil on a mould with the proper profile. Then a honeycomb of Aluminum is glued on the bended foil and then a second thin glass foil is glued on the other side of the honeycomb. Finally, a proper reflective coating is put on the outer surface of the first bended glass foil. In this way, stiff and light mirror are obtained that fulfill the requirement of the Cherenkov Telescopes. This technique was developed by INAF-Osservatorio Astronomico di Brera in collaboration with the Media Lario s.r.l. and successfully used for the MAGIC-II telescope ([15]) and then for the ASTRI telescopes ([16]). It will also be used for the MSTs at the Northern site of CTAO. This approach is based on a cost saving replica process that is very attractive for CTAO due to the multiplicity of the mirrors to be fabricated and provides lightweight mirrors with shape errors within a few microns, fully satisfying the requirements.

The secondary mirror, M2, is based on a monolithic substrate of 1.8 m diameter realised with the hot-slumping technique. A mandrel with the proper shape is put inside an oven with a flat glass foil on top; under high temperatures, the glass foil will bend and take the shape of the mandrel. The M2 Mirror is mounted on the M2 Support that allows tip/tilt/piston adjustment to fine-tune the entire SST telescope optical system alignment. This approach has already been well proven with the implementation of the ASTRI-Horn and the first ASTRI mini-array telescope. For a full description of the alignment of the segmented mirrors, evaluation of the imaging quality and spatial resolution over the full field of view of the ASTRI optical configuration see [6], this same configuration that will be adopted also for the SST.

2.4 The Cherenkov camera

The SST Camera will be based on the CHEC-S prototype, shown in Figure 6. The camera contains 2048 pixels tiled in the focal plane to sufficiently approximate the radius of curvature of 1 m resulting from the telescope optics. A scheme of the core camera architecture is shown in Figure 7, whilst an overview of current SST Camera CAD is shown in Figure 8.

The camera contains 32 SiPM tiles. Each tile contains 64 pixels of active size 6 mm x 6 mm. The chosen SiPM technology is 50 μm , “LVR3”, provided by Hamamatsu Photonics. To minimise optical cross-talk, each SiPM will be used uncoated. SiPM testing is ongoing, but sample tests indicate a peak PDE of >50% with an optical cross talk of ~5% at the intended operating voltage. SiPM tiles are mounted into a machined aluminum focal plane plate, which is liquid-cooled to stabilise the operating temperature of the SiPMs. In addition, four temperature sensors are included per SiPM tile. Dedicated electronics is mounted in the focal plane directly behind the SiPM tiles to provide individual bias control and signal amplification to each pixel.

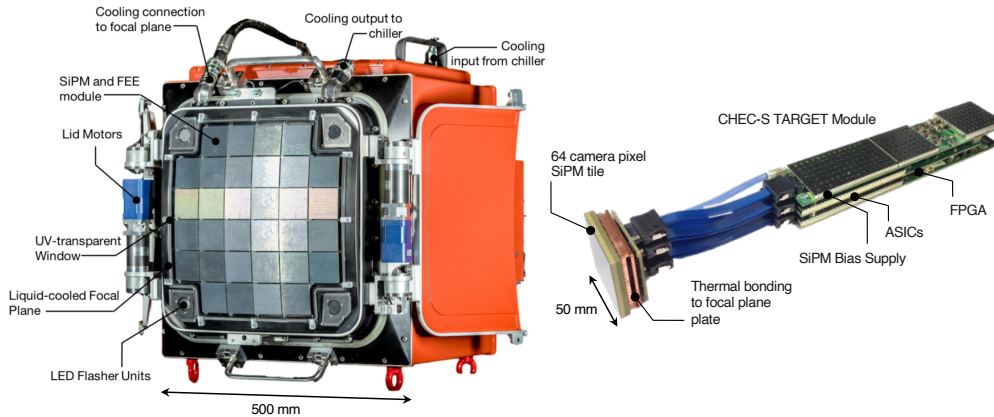


Figure 6: CHEC-S prototype camera (left) and camera readout chain (right).

A mechanical rack connects to the focal plane plate and houses 32 readout modules, based on TARGET Application Specific Integrated Circuits (ASICs), and maps 1:1 to each SiPM tile. These TARGET modules provide waveform digitisation and a first-level camera trigger. The prototype TARGET modules as used in CHEC-S are shown in Figure 6 (right). Four 16-channel CTC (CTA-TARGET-C version) ASICs provide sampling, whilst four 16-channel CT5TEA (CTA-TARGET-5TEA version) ASICs are used for triggering. The CTC ASIC is a 12-bit device that provides an effective dynamic range of 1 to ~500 photoelectrons as configured for the SST Camera. The offline recovery of larger signals is possible thanks to the waveform digitisation. The sampling rate of CTC is tuneable but nominally set to 1 GSa/s. The size of the readout window digitised from the storage array is settable in 32 ns blocks, nominally set to 96 - 128 ns to capture high-energy, off-axis events as they transit the focal plane. The first level trigger consists of summing the analogue signal from four neighbouring pixels (to form a 'superpixel') and then placing a configurable threshold on this sum, resulting in a digital output per superpixel.

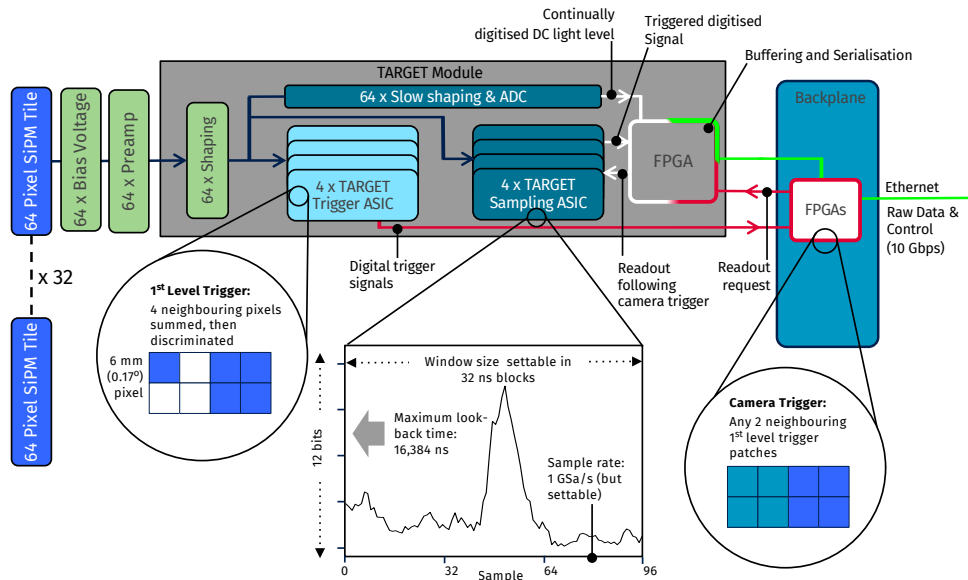


Figure 7: The core features of the SST Camera, including an overview of the trigger and digitisation scheme. For simplicity, the LED flasher, timing, and slow-control systems are excluded.

A slow-signal digitisation chain is also included in the TARGET modules. It provides a continuous (i.e., independent of the camera trigger) per-pixel measurement of the DC light level that is included to track the pointing of the telescope via stars during regular operation. A Field Programmable Gate Array (FPGA) on-board each module is used to configure the ASICs and other components, read-out raw data from the ASICs, and package and buffer raw data for output from the module.

The 32 TARGET modules are connected to a single backplane that provides the interface for power, clock, trigger, and data interface. The backplane forms a nanosecond-accurate camera trigger by combining the 512 superpixel digital trigger signals (nominally set to require a coincidence between two neighbouring superpixels). Following a camera trigger, a serial message containing a unique event identifier is sent to the TARGET modules to retrieve data from the sampling ASICs at the appropriate position in their memory. Data and communication links to the TARGET modules are routed to the backplane and amalgamated into a 10 Gbps link in an FPGA, then connected off-camera via fibre-optic cable. The full 512-bit camera trigger pattern is also sent on an even-by-event basis. An array-wide White Rabbit system connected to a timing board inside the camera provides absolute timing.

The camera is housed in an aluminum enclosure, resulting in a total size of 570 mm x 570 mm x 500 mm and a mass of ~90kg. An entrance window and external door system protect from the environmental elements. The entrance window features a multi-layer coating that acts as a bandpass between 290 – 550 nm to minimise the amount of night-sky background light (that constitutes the overwhelming source of background photons) while maximises the transmission of Cherenkov light. The camera includes an illumination system to provide calibration via fast, variable intensity LED flashes. This system contains multiple LEDs fibres coupled to three locations: a leaky fiber running around the inside of the focal plane (to illuminate the SiPMs with the camera doors closed), a diffuser in the focal plane pointed at the telescope M2 (to illuminate the camera via reflection from M2), a diffuser placed at the center of M2 pointed at the camera (to illuminate the camera directly). Based on a μ -processor, a slow control board is responsible for door control, power distribution / control, communication to the LED flasher board and backplane, and environmental monitoring inside the camera. Connection to the slow board is via a dedicated 1 Gbps link, physically contained in the same multi-fibre cable used for raw data transmission.

Thermal control of the camera is via an external chiller. Chilled liquid is circulated through the camera focal plane plate and a thermal exchange unit on the camera body. Fans internal to the camera circulate the resulting cooled air. The camera is hermetically sealed and a breather-desiccator is used to maintain an acceptable level of humidity and atmospheric pressure.

The camera, along with all required documentation and software, will be delivered as an in-kind contribution to CTAO by the SST Camera Project under the supervision of the SST Program Office. The camera project consists of 11 institutes located in: Germany, UK, Netherlands, Japan and Australia. MPIK, DESY and the University of Leicester respectively provide a camera project manager, lead systems engineer and quality manager for the project.

The camera design will be finalised and verified through a series of engineering units. Currently, individual camera modules, consisting of a single SiPM, coupled to a TARGET module are being produced. A quarter backplane (capable of housing 8 camera modules) has been built and is being used to develop the FPGA firmware. All mechanical aspects, including the coated window, have been designed and are being qualified and then produced. Mechanical and environmental tests of a full enclosure are expected to take place in Q3 2022. A quarter camera (including all mechanics, slow control board, 8 camera modules, and quarter backplane) will be assembled and tested in early 2023. The final stage in camera development is a full engineering camera (ECAM), which will be produced once all elements have individually been verified. ECAM is anticipated to be built and tested in 2023. Once lab tests are complete, ECAM will be deployed on a prototype telescope structure for on-sky verification.

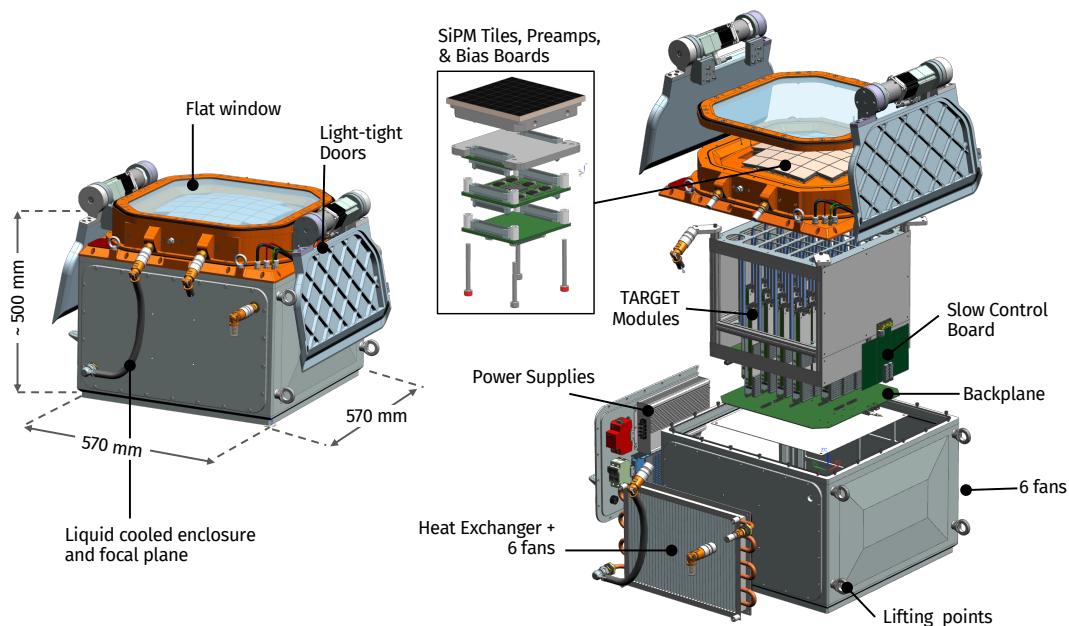


Figure 8: Overview CAD model of the SST Camera.

3. THE SST EXPECTED OVERALL PERFORMANCES

In Figure 9 we show the geometrical area as a function of the off-axis angle for a single SST telescope. The values are reported starting from the primary mirror geometrical area down to the final telescope one by considering the various vignetting effects. As can be seen, the final geometrical area is always above the 6 m^2 up to ~ 4.5 degrees off-axis in full compliance with the CTAO requirements.

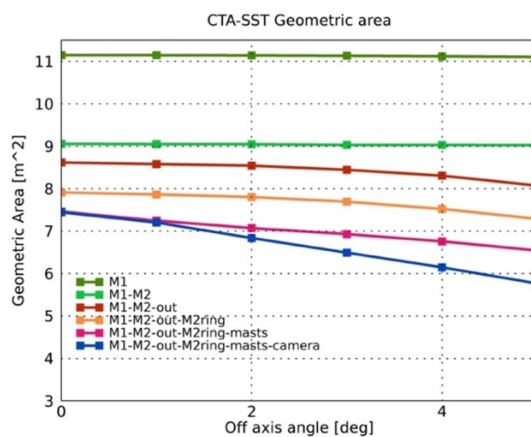


Figure 9 The geometrical area of an SST telescope as a function of the off-axis angle in degrees. The different curves show the decreasing area due to the vignetting of various telescope components up to the focal plane camera. In particular: the top line provides the geometrical area of the primary mirror M1, the next line includes the vignetting due to the obscuration of the secondary mirror M2, the next line includes the vignetting due to the photons that are reflected by M1 but are not intercepted by M2, the next line includes the vignetting due to the mechanical structure mounted around and on top of the M2, the next line includes the vignetting due to the mechanical structure that support both M2 and the camera and the final one includes the vignetting due to the camera.

The on-axis performances of the SST array between 0.2 to 100 TeV is shown in Figure 10 both for 37 and 42 SST telescopes; note that the SST sensitivity will go up to 200 TeV and beyond even though in this figure, the sensitivity curve is shown only up to 100 TeV. This sensitivity curve is based on the current and final array layout that has been the result of a thorough optimization process that is described in detail in [17]. The performance of the array layout were derived from Monte Carlo simulations and produced by using the Eventdisplay software [18]. The Monte Carlo simulations of extensive air showers and the Cherenkov light they induce were generated by using the CORSIKA program (version 7.7100) [19] and then the Cherenkov photons from the air shower are propagated through the telescopes using the sim_telarray simulation package (version 2020-06-28) [20].

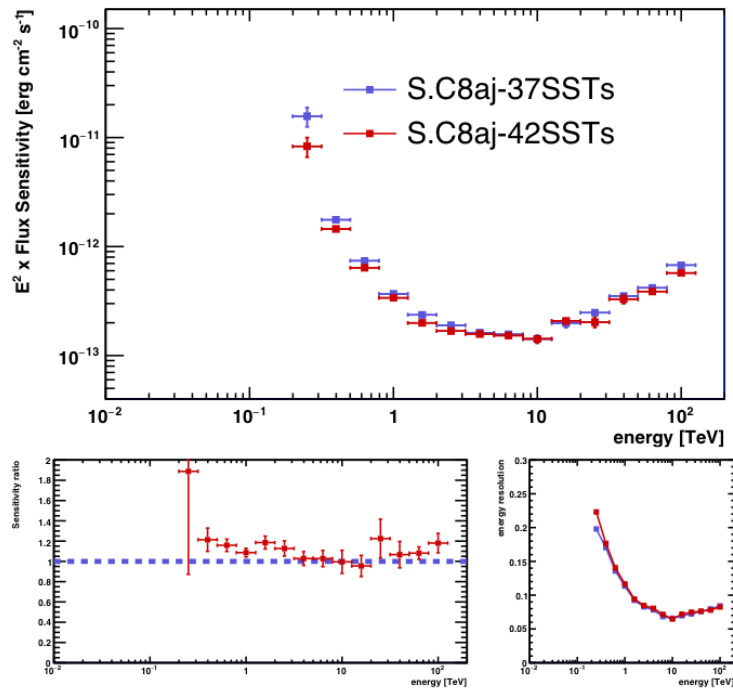


Figure 10 The on-axis differential sensitivity of the SST array (for 37, blue, and 42, red, telescopes) for 50 hours of observations as a function of the energy between ≈ 0.2 TeV and ≈ 100 TeV (top panel). The left bottom panel compares the sensitivity between the two configurations of 37 and 42 telescopes. The bottom right panel shows the energy resolution as a function of energy (Courtesy to CTAO).

4. CONCLUSIONS

An SST international consortium has been established to deliver the SST array as an in-kind contribution to CTAO. This is based on a well-defined and solid design that has been proven and consolidated through the construction of prototypes both for the telescope structure and for the focal plane camera. The program is now going through a Bridging phase that started on July 2021 and will end in December 2022. During this phase the SST design will be finalised in compliance with the CTAO interfaces and requirements. This phase will be concluded with a formal review to verify the design against CTAO requirements, before proceeding with the consolidation and production phases.

The next steps will be the consolidation of the serial production of the SST structure and optics involving also commercial partners in Europe that will be selected via public bids. All components produced will undergo quality control and product compliance under the strict supervision of our team before shipment to the CTAO Southern site. The cameras are developed, assembled and tested by the participating institutes. They will undergo functional and verification tests before shipment.

The current schedule foresees the realisation of the first full telescope structure ready to be shipped to Chile in early 2024. On the same time scale, it is foreseen the development of the first SST camera, while the completion of the full SST array is expected to occur by 2027.

ACKNOWLEDGMENTS

We gratefully acknowledge financial support from the agencies and organizations listed here: <http://www.cta-observatory.org/consortium>. We thank the EIE GROUP Srl and the Media Lario Srl Companies for their support and contributions to the study and development of the SST project.

REFERENCES

- [1] Wild, W., Ferrini, F., “CTAO – the world’s first and largest ground-based gamma-ray observatory”, SPIE this conference (2022)
- [2] Mazin, D., Cortina, J., Teshima, M., “Large Size Telescope Report”, AIPC proc, Vol. 1792, issue 1 (2016) arXiv: 1610.04403
- [3] Garczarczyk, M., “The Medium-Sized Telescopes of the CTAO”, SPIE this conference, (2022)
- [4] Pareschi, G., Proc SPIE9906, 99065T (2016)
- [5] Watson, J.J. and Zorn, J., “Commissioning and performances of CHEC-S – a compact high-energy camera for the Cherenkov telescope Array, ICRC2019 vol. 36, 821 (2019) arXiv: 1907.09252
- [6] Giro, E., et al., “First optical validation of a Schwarzschild Couder telescope: the ASTRI SST-2M Cherenkov telescope”, A&A 608, A86 (2017)
- [7] Lombardi, S., et al., “First detection of the Crab Nebula at TeV energies with a Cherenkov telescope in a dual-mirror Schwarzschild-Couder configuration: the ASTRI-Horn telescope”, A&A 634, A22 (2020)
- [8] White, R., et al., “The Small-Sized Telescopes for the Southern Site of the Cherenkov Telescope Array”, 37th ICRC conference, Berlin, Germany (2021) arXiv: 2110.14527
- [9] Vassiliev, V., et al., “Wide field aplanatic two-mirror telescopes for ground-based γ -ray astronomy”, *Astroparticle Physics* 28, 10-27 (2007)
- [10] Pareschi, G., “The ASTRI SST-2M prototype and mini-array for the Cherenkov Telescope Array (CTA)”, proc. SPIE, vol. 9906, 99065T (2016)
- [11] Scuderi, S., et. al, “The ASTRI Mini-Array of Cherenkov telescopes at the Observatorio del Teide”, JHEA 35, 52 (2022)
- [12] Marchiori, G., et al., “ASTRI SST-2M: the design evolution from the prototype to the array telescope”, Proc. SPIE vol. 10700, 107005W (2018)
- [13] Dournaux, J.-L., Bouley, F., Rébert, E., Huet, J.M., Sol H., et al., "Mechanical optimization of the M1 Dish of the CTA-SST, the SST of the future Cherenkov Telescope Array," Proc. SPIE, (2022).
- [14] Sironi, G., “Aplanatic telescopes based on Schwarzschild optical configuration: from grazing incidence Wolter-like X-ray optics to Cherenkov two-mirror normal incidence telescopes”, Proc. SPIE 10399, 1039903 (2017)
- [15] Canestrari, R. et al., “The ASTRI SST-2M prototype for the next generation of Cherenkov telescopes: structure and mirrors”, Proc. SPIE 8861, 886102 (2013)
- [16] La Palombara, N., et al., “Mirror production for the Cherenkov telescopes of the ASTRI mini-array and the MST project for the Cherenkov Telescope Array”, JATIS vol. 8, id. 014005 (2022), arXiv: 2201.08103
- [17] Gueta, O., et al., “The Cherenkov Telescope Array: layout, design and performance”, PoS(ICRC2021)885 (2021), arXiv: 2108.04512
- [18] Maier, G., Holder, J., “Eventdisplay: an analysis and reconstruction package for ground-based gamma-ray astronomy”, ICRC2017 Vol. 301, id.747 (2017), arXiv: 1708.04048
- [19] Heck, K., et al., “CORSIKA: a Monte Carlo code to simulate extensive air showers”, Tech. Rep. FZKA 6019, Forschungszentrum Karlsruhe (1998)
- [20] Bernlöhr, K., “MC simulation and layout studies for a future Cherenkov Telescope Array”, *Astroparticle Physics*, 30, 149 (2008)